8-11

Vessel Segmentation in Angiograms using Hysteresis Thresholding

Alexandru-Paul Condurache
University of Luebeck,
Institute for Signal Processing
Ratzeburger Allee 160,
D-23538 Luebeck, Germany
condura@isip.uni-luebeck.de

Til Aach
RWTH Aachen University,
Institute of Image Processing and Computer Vision
Templergraben 55,
D-52056 Aachen, Germany
aach@isip.uni-luebeck.de

Abstract

Angiography (i.e. vessel imaging after the injection of a radiopaque substance) is a widely used procedure for vessel observation in both clinical routine and medical research. Often for the subsequent analysis of the vasculature it is needed to measure the angiogram area covered by vessels and/or the vessel length. For this purpose we need vessel enhancement and segmentation. While there are already many organ specific vessel segmentation algorithms, we propose in this contribution a more general method which includes a Hessian supported vessel enhancement step followed by segmentation based on the hysteresis threshold paradigm.

1 Introduction

The angiography supported analysis of the vasculature of different organs is a task frequently encountered in clinical routine and medical research.

For instance, the success of a skin transplant depends on the proper revascularization of the transplanted dermal matrix. To promote angiogenesis different drugs may be administered. The efficiency of such a drug treatment has been evaluated in laboratory experiments on rats using micro-angiograms of the transplant area [1]. Towards this end the newly grown vessels need to be segmented to allow the quantification of the area which they cover and also the vessel length.

Proliferative diabetic retinopathy is characterized by neovascularization (the growth of new blood vessels). Evaluating the vessel covered area during a retina examination (imaged e.g. by fluorescin angiography or fundus photography) is instrumental in diagnosis. For a proper measurement we need vessel enhancement and segmentation [2].

Also, recent algorithmic developments in the field of computer supported heart vessel interventions underline the need for a coronary vessel tree area related feature [3], [4]. One way to extract such a feature is by counting the vessel pixels in a segmentation result.

Vessel segmentation algorithms typically follow a two-step approach [5], i.e. feature extraction followed by segmentation. In most cases feature extraction is actually a vessel enhancement step which uses e.g. matched filters [6], the eigenvalues of the Hessian matrix at different scales [7] or other methods [5]. One exception is the article by Staal [2] where several pixel features are extracted and then the best pixel feature set is obtained by sequential forward selection.

Vessel segmentation can be carried out in a supervised manner based on a pre-labeled set of examples e.g. using k-nearest neighbor classification [2] or in an unsupervised manner e.g. by active contours [8] or tracking [9] as well as by other methods [10].

We also distinguish between fully automatic [2], [9] and semiautomatic algorithms [8] where the latter typically require some user supplied information to achieve a correct result.

Another characteristic of existing vessel segmentation algorithms is that they are not only imaging modality specific (which is in general unavoidable) but also organ specific. In this contribution we propose a more general, automatic, unsupervised method for segmenting vessels in angiograms (and angiogram-like images) to support vasculature analysis tasks such as e.g. vessel area and vessel length measurements. We start by enhancing the vessels obtaining a vessel map where we select the vessel pixels by hysteresis thresholding.

2 Vessel enhancement

In the light of our segmentation task, the purpose of vessel enhancement is to obtain two separable vessel/background pixel classes. There are two aspects which define separability and which guide our vessel enhancement: (i) a small intra-class variance which implies a homogeneous gray level representation for each class and (ii) a large inter-class variance which means a prominent contrast.

Enhancement is then based on the observation that vessels are tubular structures of a certain size which appear darker than their immediate surroundings in the analyzed images.

In a first step we select only dark image structures of a certain size by means of a morphological Tophat filter [11]. This filter is defined as the difference between the original image and its closing. Choosing the size of the closing window slightly larger than the largest vessel diameter will suppress vessels while keeping the background. The subsequent subtraction of this result from the original image yields then predominantly vessel information while removing the background. The Tophat filter, though not a genuine contrast enhancer, (as the difference between vessel pixels and the background remains unchanged) increases the separability between the two pixel classes mainly by reducing the variance of the background. An example is shown in Figure 2b.

The vessel pixel class naturally exhibits a rather large variance as the vessel contrast depends on the vessel size via the received contrast agent quantity. In the vessel map

we seek to reduce this variance by enhancing the vessels similarly irrespective of their size. For this purpose, we analyze the largest eigenvalue of the Hessian matrix which responds to the presence of a valley (i.e. vessel) on the image function by taking prominent values [7].

The size of the vessels to which the eigenvalue is sensitive depends on the image scale. Thus, in a second enhancement step, while varying the scale stepwise, we compute the eigenvalue image each time and combine the results pixelwise across the scales by the maximum rule. A final enhancement result is shown in Figure 2c.

3   Segmentation

To segment the vessels we use a hysteresis threshold. This is a physically motivated concept which translates in computer vision in a bi-threshold procedure typically used for two class object-background pixel segmentation [12]. The image is first segmented by a 'hard' threshold which yields only high confidence object pixels (thus also many false negatives). A second threshold operation, this time with a 'weak' threshold, returns then the entire object together with many background pixels (i.e. many false positives). Using prior knowledge with respect to object connectivity, the segmentation is achieved by choosing from among the object pixels selected by the 'weak' threshold only those pixels connected to a high confidence one. A nearly correct segmentation is thus achieved despite the potential overlap of the class conditional probability density functions.

We have investigated two different methods to compute the thresholds needed. The first uses hypothesis testing while the second is an empirically motivated percentile based rule.

3.1   Hypothesis testing

The 'hard' threshold can be set using the background class conditional probability density function (pdf) by means of a significance test. The null hypothesis is that the pixel under investigation belongs to the background class. To obtain the threshold we choose a small significance level. We have then:

$$\int_{-\infty}^{t_h} p\,(\,x \mid \omega_{b}\,) \,=\, \alpha$$

with t_h the threshold, ω_b the background class, x the pixel gray-level and α the significance.

If the gray level of an investigated pixel is below this threshold then the probability of it belonging to the class background is very small (i.e. less than the significance) which means that the available data does not sustain the null hypothesis in that case. As on the vessel map we have either background or vessel pixels, then the pixel under consideration must belong to the vessel class. The error probability of this decision (i.e. the type I error probability) equals the significance level. The 'hard' threshold separates thus high confidence vessel pixels from the rest.

The 'weak' threshold can be set using the vessel class conditional pdf. This time we hypothesize that the pixel under consideration is a vessel pixel. To compute the threshold, we impose that the error probability for a decision in agreement with our hypothesis is very small:

$$\int_{t_w}^{\infty} p\,(\,x \mid \omega_{v}\,) \,=\, \beta$$

with t_w the threshold, ω_v the vessel class, x the pixel gray-level and β the error probability.

If the gray level of the investigated pixel is above this threshold this means that the probability of it belonging to class vessel is very small and again as there are only two classes on the vessel map, it must belong to the background class. Thus, the 'weak' threshold separates high confidence background pixels from the rest.

3.2   Estimating the probability density function

The class conditional pdfs needed for the thresholds' computation can be estimated provided some samples from each density are known. We find these samples by means of an unsupervised histogram segmentation algorithm first proposed by Otsu in [13].

Thus, if we assume some generic form of the distribution its parameters can be determined using the maximum likelihood or the maximum a posteriori estimation. Such a parametric estimation has some disadvantages e.g.: (i) it is considered that the random variable can take values in an infinite interval and then the computed thresholds may fall outside the vessel map's range, (ii) assuming a generic distribution form limits the flexibility of our approach providing thus an additional source for errors if the assumption is incorrect or if the samples used at estimation were not uniformly extracted.

If no assumptions are made with respect to the distribution's generic form then it can be found e.g. using Parzen estimation [14]. The pdf at a certain position $\hat{y}$ is then computed as:

$$\widetilde{p}\,(\,\hat{y} \mid \omega\,) = \frac{1}{N_\omega} \sum_{i=1}^{N_\omega} \gamma\,(\,\hat{y} - y_i\,)$$

with N_ω the number of available samples y_i for class ω and γ the kernel potential function or Parzen window. A function should satisfy certain conditions to be a kernel. In our experiments we have used two kernels: the Gaussian kernel:

$$\gamma(z) = \frac{1}{\sqrt{2\pi}h} e^{\left(-\frac{z^2}{2h^2}\right)}$$

and the exponential kernel:

$$\gamma(z) = \frac{1}{2h} e^{\left(-\frac{|z|}{h}\right)}$$

where h is the size of an interval with midpoint $\hat{y}$.

This nonparametric estimation procedure is more flexible than the parametric one and the thresholds remain practically always in the vessel map range if the parameter h is properly chosen (empirically $h < 5$). However the better performance is balanced by a severe increase in the time needed to compute the thresholds.

3.3   Fast selection of thresholds

To compute the thresholds faster we propose an empirically motivated rule. To derive this rule we use the observations that: (i) the 'hard' threshold separates high confidence vessel pixels from the rest, (ii) the 'weak' threshold separates high confidence background pixels

from the rest and (iii) the vessels in the vessel map are characterized by gray levels darker than those characterizing the background.

Then, the two thresholds are computed using percentiles by specifying how much of the image surface is *certainly* occupied by vessel and background pixels respectively. This procedure is illustrated in the next figure:
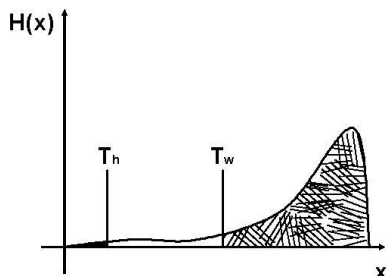

Figure 1.   Vessel map histogram with thresholds.

The black area under the histogram corresponds to the image surface *certainly* covered by vessels. The percentile enclosing it gives the 'hard' threshold T_h The dashed area under the histogram corresponds to the image surface *certainly* covered by background. This implies that on what remains of the image we should find virtually all the vessel pixels. Thus, the 'weak' threshold T_w is given by a percentile corresponding to: 100% minus the percentage of the image surface *certainly* covered by background. Then practically, T_h selects *only* vessels pixels and T_w *all* vessel pixels.

4   Experiments and Results

To test our segmentation algorithm we have used three image sets: one publicly available retina images data base with 20 images [2], 11 skin transplant micro-angiograms and six coronary angiograms. From the retina images only the green channel was used. The ground truth is given by hand segmentations. For the skin transplant micro-angiograms and for the coronary angiograms the manual segmentations were done by the first author. The retina data base has also hand segmentation results done by two observers (set A and set B). The results obtained by the first observer are considered closer to the absolute truth. All images were 512x512 pixels large. For the retina images this size was obtained by appropriately ignoring the image margins. We measured the quality of our vessel map by the J_1 separability criteria as described in [15, p. 446]. For comparison we measured also the separability of the original image and of a simple Tophat filter result. The Tophat filter's window size was: for retina images 9x9, for micro-angiograms 13x13 and for coronary angiograms 21x21 pixels. The images were decomposed on a Gaussian pyramid with two levels. To prevent noise boosting the images were low-pass filtered before computing the Hessian matrix. Table 1 gives the separability measured for the 20 retina images. The results are mean values over all images. As ground truth the segmentation given by the first observer are used.

Table 1.   Separability (the higher the better).

Original image	Tophat result	Vessel map
0.0723	0.4730	0.6325

One vessel map example is shown in the next figure together with the original image and a Tophat filtration result.
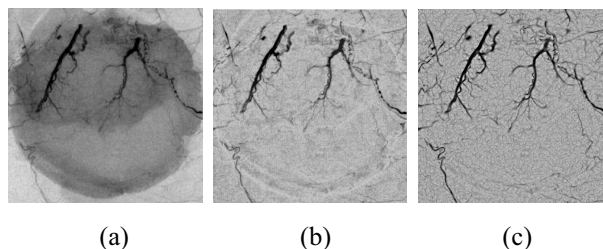

| (a) | (b) | (c) |

Figure 2. Original skin transplant micro-angiogram (a), Tophat result (b) and vessel map (c).

To measure the performance of our segmentation algorithm we have computed the area under the receiver operating characteristic (ROC) curve [14]. This performance measure was also used to find the optimal parameters set (i.e. percentages of image area certainly covered by vessels and background respectively). The ROC curve for the retina images is shown in the next figure:
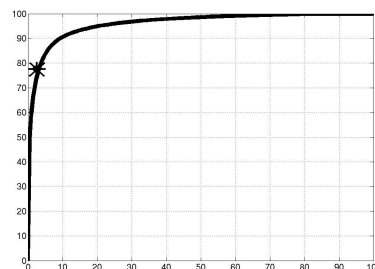

Figure 3.   ROC curve for the retina images. Y-axis: true positives (%), X-axis : false positives (%)

The curve was computed by setting the percentage of image area certainly covered by vessels to six percents and varying the percent of image surface certainly covered by background between one percent and 100% in unit steps. To find the 'weak' pixels connected to a 'hard' one we use an 'eight' (square) neighborhood. The area under the ROC curve was 0.9643. Each point on the curve represents the mean percentage of true and false positives over all test images. The star marks the results obtained when comparing set B to set A. Its coordinates are 2.29 % false positives and 77.73% true positives. The point on the ROC curve closest to these coordinates was obtained when 87% of the image surface was covered by background. In this case the percentage of false positives was 3.21 and that of true positives was 77.72. Similar results were obtained when computing the thresholds by non-parametric hypothesis testing with the following parameters: $\alpha = 5 \cdot 10^{-4}$, $\beta = 5 \cdot 10^{-2}$, $h = 2$, and a 'Gaussian' type of kernel. On a Pentium IV PC at 2.1 GHz with 512 MB memory under Matlab it took less than 10 seconds to segment an image using the fast threshold selection method (including vessel map computation) and approximately 30 minutes to segment an image with the nonparametric hypothesis testing method.

In Table 2 we show results (true and false positives rates) obtained for each of the three image sets: retina images, micro-angiograms and coronary angiograms. For comparison the results obtained by Otsu thresholding are also given.

Table 2. Segmentation results.

	retina		skin		coronary	
	Hyst.	Otsu	Hyst.	Otsu	Hyst.	Otsu
TP (%)	77.72	49.11	80.61	57.38	72.40	55.21
FP (%)	3.21	0.51	4.63	3.51	3.55	8.60

The parameters used were (in percents of image surface certainly covered by vessels and background respectively): six and 87 for the retina images, three and 85 for the skin transplant micro-angiograms and 0.1 and 84 for the coronary angiograms. In the next figure segmentation results obtained for a retina image (first row, parameters: six and 82), a skin transplant micro-angiogram (second row) and a coronary angiogram (third row) are shown. The first column shows the original image, the second the ground truth and the third the segmentation result.
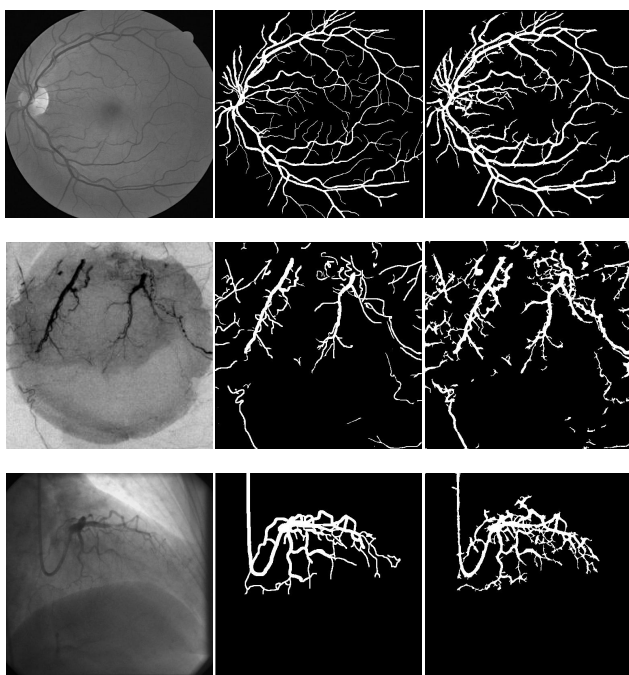

Figure 4. Segmentation results.

5 Discussion

The results show that the method we have described here performs well while at the same time being general enough to be applicable to a wide range of angiograms irrespective of the organ whose vasculature is imaged. The results obtained for retina vessel segmentation are comparable with other modern methods on similar data sets [2]. The performance of our method depends crucially on the quality of the vessel map. The vessel map was specially designed to increase the separability. Its main feature is that it enhances vessels in a similar manner irrespective of their size. This is achieved mainly by analyzing the vessels in a multiresolution decomposition with the largest eigenvalue of the Hessian matrix and combining the results by the maximum rule. We have described two methods to compute the hysteresis thresholds. The first method is well anchored in the statistical theory but it is also time demanding. The second method is rather a heuristic approach but it is fast and it yields good results. For a successful segmentation a certain degree of interaction is needed. One has to correctly set the Tophat window size

and the percentages of image surface covered by vessels and background respectively.

6 Conclusions

We have described in this contribution a segmentation algorithm for vessel analysis tasks such as surface and/or length measurements in angiograms and angiogram-like images. Our method is general and thus widely applicable. Vessel-like structures larger than the vessel size are eliminated by the Tophat filter and then the vessels are enhanced by analyzing the largest eigenvalue of the Hessian matrix. The segmentation is done by hysteresis thresholding. The two thresholds needed are computed by a fast percentile rule. Our method is fast and performed well on the test images. We intend to report results obtained on a larger data set in the near future.

References

[1] S. Grzybowsky, B. Bucsky et al: "A microangiography technique to quantify fascicutaneous blood vessels in small laboratory animals," *LAS*, vol.389, no.10, 2004.

[2] J. Staal, M. D. Abramoff et al: "Ridge-based vessel segmentation in color images of the retina," *IEEE TMI*, vol.23, no.4, pp.501-509, 2004.

[3] T. Aach, A. Condurache et al: "Statistical-model based identification of complete vessel tree frames in coronary angiograms," *EI 2004*, SPIE vol.5299, pp.283-294, 2004.

[4] A. Condurache, T. Aach et al: "Fast detection and processing of arbitrary contrast agent injections in coronary angiography and fluoroscopy," *BVM 2004*, pp.5-9, Springer 2004.

[5] C. Kerbas and F.K.H. Quek: "A review of vessel extraction techniques and algorithms," http://vislab.cs.vt.edu/review/

[6] R. Poli and G. Valli: "An algorithm for real time vessel enhancement and detection," *CMPB*, vol.52, no.1, pp.1-22, 1997.

[7] A. F. Frangi, W. J. Niessen et al: "Multiscale vessel enhancement filtering," *MICCAI LNCS*, vol.1496, pp.130-137, 1998.

[8] R. Toledo, X. Orriols et al: "Eigensnakes for vessel segmentation in angiography," *Proc. of ICPR*, pp.340-343, 2000.

[9] Z. Chen and S. Molloi: "Multiresolution vessel tracking in angiographic images using valley courses," *OE*, vol.42, pp.1673-1682, 2003.

[10] X. Jiang and D. Mojon: "Adaptive local thresholding by verification based multithreshold probing with application to vessel detection in retinal images," *IEEE TPAMI*, vol.25, no.1, pp.131-137, 2003.

[11] E. R. Dougherty: "Mathematical morphology in image processing," *Marcel Dekker*, 1992.

[12] J. Canny: "A computational approach to edge detection," *IEEE TPAMI*, vol.8, no6, 1986.

[13] N. Otsu: "A threshold selection method from gray-level histograms," *IEEE TSMC*, vol.9, no.1, pp.62-66, 1979.

[14] C.W. Therrien: "Decision, estimation, and classification," *John Wiley*, 1989.

[15] K. Fukunaga: "Introduction to statistical pattern recognition," *Academic Press*, 1990.